Title

Tuning magnetotransport in PdPt/Y3Fe5O12: Effects of magnetic proximity and spin-orbit coupling

Journal

Applied Physics Letters, 105(1)

ISSN

0003-6951

Authors

Zhou, X

Ma, L

Shi, Z

et al.

Publication Date

2014-07-07

DOI

10.1063/1.4890239

Tuning magnetotransport in PdPt/$Y_3Fe_5O_{12}$: Effects of magnetic proximity and spin-orbit coupling

X. Zhou,[1] L. Ma,[1] Z. Shi,[1] G. Y. Guo,[2,a)] J. Hu,[3] R. Q. Wu,[3] and S. M. Zhou[1,b)]
[1]*Shanghai Key Laboratory of Special Artificial Microstructure and Pohl Institute of Solid State Physics and School of Physics Science and Engineering, Tongji University, Shanghai 200092, China*
[2]*Department of Physics, National Taiwan University, Taipei 10617, Taiwan*
[3]*Department of Physics and Astronomy, University of California, Irvine, California 92697-4575, USA*

(Received 12 June 2014; accepted 2 July 2014; published online 10 July 2014)

We report that anisotropic magnetoresistance (AMR) and anomalous Hall conductivity (AHC) in the $Pd_{1-x}Pt_x/Y_3Fe_5O_{12}$ (YIG) bilayers could be tuned by varying the Pt concentration (x) and also temperature (T). In particular, the AHC at low T changes its sign when x increases from 0 to 1, agreeing with the negative and positive AHC predicted by our *ab initio* calculations for the magnetic proximity (MP)-induced ferromagnetic Pd and Pt, respectively. The AMR ratio is enhanced by ten times when x increases from 0 to 1. Furthermore, the AMR of PdPt/YIG bilayers shows similar T-dependence as the magnetic susceptibility of the corresponding bulk Pd/Pt, also indicating the MP effect as the origin of the AMR. The present work demonstrates that the alloying of Pt and Pd not only offers tunable spin-orbit coupling but also is useful to reveal the nature of the AMR and AHC in Pt/YIG bilayers, which are useful for spintronics applications. © *2014 AIP Publishing LLC*.
[http://dx.doi.org/10.1063/1.4890239]

Generation, manipulation, and detection of pure spin current are an active research topic because of the need of low Joule heat production in spintronic devices.[1–4] By the spin Hall effect, the pure spin current can be obtained in semiconductors via strong Rashba and Rashba-Dresselhaus spin-orbit coupling (SOC). By the spin Seebeck effect (SSE), it can also be produced in ferromagnetic materials with a temperature gradient and injected into another nonmagnetic layer across the interface. In general, the pure spin current cannot be probed by conventional electric approaches. Instead, it manifests through the inverse spin Hall effect.[5,6]

With the strong SOC in the Pt layer and the low magnetic damping in the $Y_3Fe_5O_{12}$ (YIG) insulating layer, Pt/YIG bilayers are ideal for generating pure spin currents in spintronic devices.[7–16] However, the SSE and the anomalous Nernst effect in the Pt/YIG systems were argued to be entangled.[8] Since the latter comes from the spin polarization of the nearly ferromagnetic Pt layer induced by the magnetic proximity (MP) effect, many attempts have been made to distinguish the MP effect in the Pt/YIG system. As the magnetic moment of the Pt layer is too small to be measured by the conventional magnetometry, the anisotropic magnetoresistance (AMR), and anomalous Hall effect (AHE) have been adopted for varying thickness of the Pt layer and sampling temperature (T).[9–15] Up to date, magnetotransport results are still controversial. The AMR ratio of the Pt/YIG system exhibits an angular dependence different from the conventional AMR in most magnetic films, which was attributed to the spin Hall magnetoresistance (SMR).[13–15] However, its nonmonotonic variation with T cannot be understood in the SMR model.[11] Moreover, the mechanism of the sign change of the AHE in the Pt/YIG system is still unclear.[8] Results of different x-ray magnetic circular dichroism (XMCD) experiments are also inconsistent.[11,17] Therefore, the mechanism of the magnetotransport phenomena in the Pt/YIG system awaits more experiments.

In this work, we study the AMR and AHE in the $Pd_{1-x}Pt_x$(PdPt)/YIG systems both experimentally and theoretically. Since Pd and Pt atoms are isoelectronic elements with different atomic numbers, the effective SOC strength can be substantially adjusted by changing x without much disturbance on other electronic features.[18] Indeed, we find that the AMR, anomalous Hall conductivity (AHC), and ordinary Hall coefficient (OHC) in the PdPt/YIG bilayers can be tuned in a large range by changing x and also T. Particularly fascinating is the concurrent sign changes of the AHC and OHC at low T when x increases from 0 to 1, in good agreement with the negative and positive AHC predicted by our *ab initio* calculations for the MP-induced ferromagnetic Pd and Pt, respectively. Further, the AMR ratio of the PdPt/YIG bilayers and the magnetic susceptibility χ of the corresponding bulk Pd/Pt have similar broad peaks at the same T. This work, therefore, provides a firm evidence that the AMR and AHE observed in the PdPt/YIG bilayers are caused by the MP-induced magnetization in the Pd/Pt layer. Our present finding helps to better understand the nature of the magnetotransports in the Pt/YIG system.

A series of PdPt (1 nm)/YIG (70 nm) bilayers were fabricated by pulse laser deposition and subsequent magnetron sputtering in ultrahigh vacuum on (111)-oriented, single crystalline $Gd_3Ga_5O_{12}$ (GGG) substrates. The YIG layers were epitaxially grown via pulsed laser deposition from a stoichiometric polycrystalline target using a KrF excimer laser. Subsequently, PdPt layers were deposited by magnetron sputtering. The film thickness and microstructure were characterized by using a D8 Discover X-ray diffractometer with Cu Kα radiation (wavelength of about 1.54 Å). X-ray reflection (XRR) spectra show that the thicknesses of YIG and PdPt layers were determined to be 70 ± 0.6 and

a)Electronic mail: gyguo@phys.ntu.edu.tw
b)Electronic mail: shiming@tongji.edu.cn

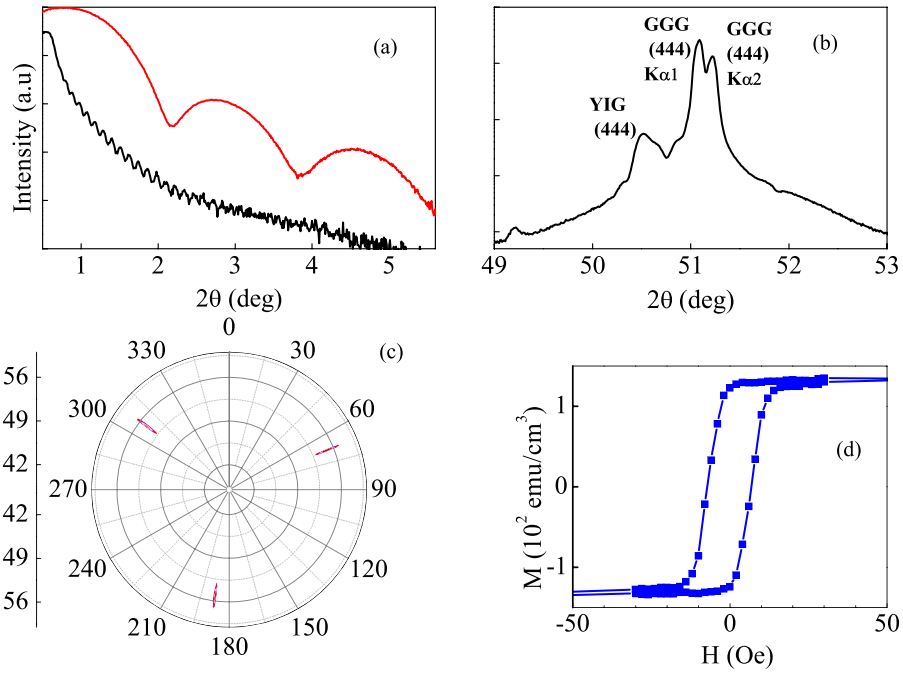

FIG. 1. For typical Pt/YIG films, XRR at small angles (a) and XRD at large angles (b), Φ and Ψ scan with fixed 2θ for the (008) reflection of GGG substrate and YIG film (c). In (d), the room temperature in-plane magnetization hysteresis loop of the YIG layer is shown. In (a), black and red lines correspond to single layer YIG film and Pt/YIG bilayers, respectively.

1.0 ± 0.05 nm, respectively, as shown in Fig. 1(a). The root mean square surface roughness of the YIG layer is fitted to be 0.6 nm. Figure 1(b) shows that the x-ray diffraction (XRD) peaks near $2\theta = 51°$ for (444) orientations of the GGG substrate and the YIG films.[19] The epitaxial growth of the YIG films was confirmed by Φ and Ψ scans with fixed 2θ for the (008) reflection of the GGG substrates and the YIG films, as shown in Fig. 1(c). In-plane magnetization hysteresis loops of the YIG films were measured at room temperature by vibrating sample magnetometer in Fig. 1(d). The saturation magnetization of 134 emu/cm^3 is almost equal to the theoretical value, and the coercivity is as small as 6.0 Oe. High quality epitaxial YIG films are therefore achieved.

The films were patterned into normal Hall bar and the transverse Hall resistivity (ρ_{xy}) and the longitudinal resistivity ρ_{xx} were measured by physical property measurement system (PPMS) as a function of H with $\theta_H = 0°$ as shown in the inset of Fig. 2(a), and then the anomalous Hall resistivity ρ_{AH} was extrapolated from the linear dependence of ρ_{xy} at large H. The slopes in the positive and negative high field regions are identical and the intercept arises from the AHE instead of the longitudinal resistivity.[20] Figure 2 shows that for Pt/YIG and Pd/YIG, the saturation field of Hall loops at both 10 K and 300 K is close to the demagnetization field of the YIG layer. For all samples and, in particular, the Pd-rich ones, the linear part of the Hall loop at high magnetic fields becomes prominent due to small intercept, i.e., ρ_{AH}, like the permalloy in which the ρ_{AH} is nearly zero due to the band-filling effect.[21] For the Pd/YIG samples, both ρ_{AH} and OHC R_0 are negative at 300 K and 10 K. In contrast, they both have opposite signs at $T = 10$ and 300 K for the Pt/YIG. As analyzed below, the SMR model can be unambiguously excluded in the explanation of the Hall loops. According to the SMR model,[13–15] one has $\rho_{xy} = \rho_{2,SMR} m_n + \rho_{3,SMR} m_j m_t + R_0 H$, where m_j, m_t, and m_n are the components of the magnetic moment in the YIG layer parallel and perpendicular to the sensing current as well as along the film normal direction, respectively. As Althammer *et al.* pointed out, the coefficients $\rho_{2,SMR}$ and

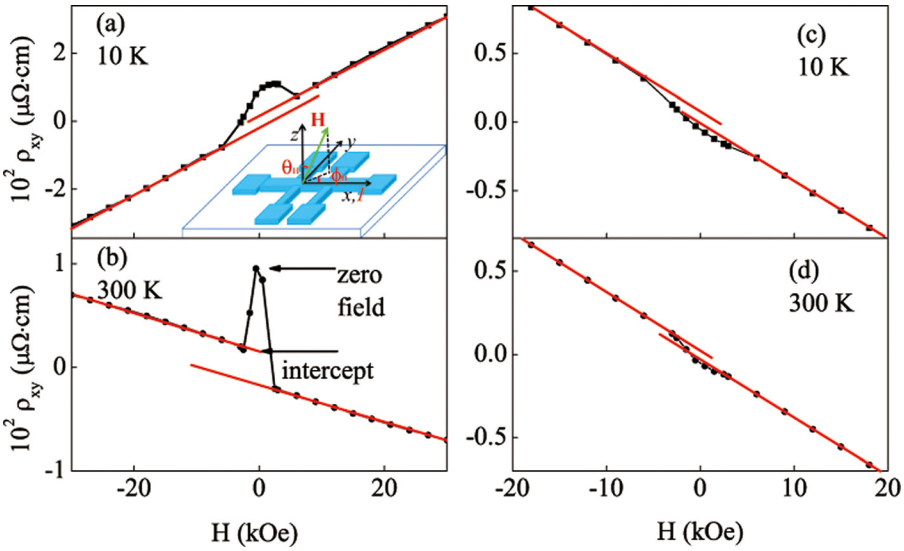

FIG. 2. For Pt (1 nm)/YIG ((a) and (b)) and Pd (1 nm)/YIG ((c) and (d)) films, the transverse Hall resistivity ρ_{xy} versus H at 10 K ((a) and (c)) and 300 K ((b) and (d)). In experiments, the H is applied along the film normal direction, i.e., $\theta_H = 0°$. The inset in (a) shows the schematic geometry of the magnetotransport measurements.

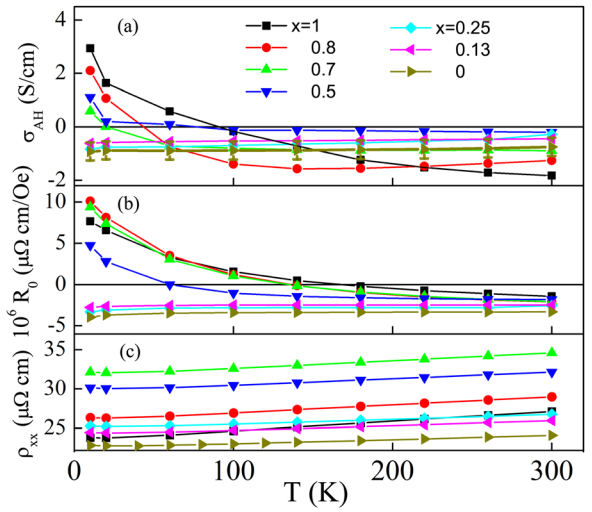

FIG. 3. For PdPt (1 nm)/YIG films, σ_{AH} (a), R_0 (b), and ρ_{xx} (c) versus T for various x. In (a), the error bars are added for $x = 0$ and 1.0.

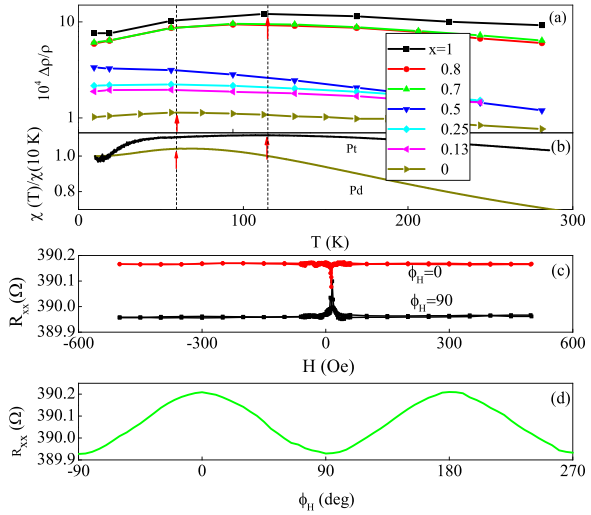

FIG. 4. For PdPt (1 nm)/YIG films, the AMR ratio versus T for various x (a). The χ versus T for bulk Pt and Pd (b). For Pt(1 nm)/YIG films, AMR curves at $\phi_H = 0°$ and 90° (c) and angular dependent AMR at $H = 10$ kOe (d). In (b), the χ was measured using small Pt and Pd pieces (mass $\simeq 0.2$ g) and at 10 K it is 2.06×10^{-5} and 8.38×10^{-5} for bulk Pt and Pd, respectively. In (c) and (d), the ϕ_H refers to the angle between the in-plane H and the sensing current. In (a), (c), and (d), $\theta_H = 90°$.

$\rho_{3,SMR}$ in the Pt/YIG are negative and positive below 300 K,[15] respectively. The extrapolated value of the ρ_{xy} at zero field should *always* be negative below 300 K.[15] We may conclude that the observed Hall loops are dominated by the AHE instead of the SMR effect. This clearly indicates the existence of the MP effect.

Figure 3 shows the σ_{AH} and R_0 as a function of T for all samples, where $\sigma_{AH} = \rho_{AH}/(\rho_{xx}^2 + \rho_{AH}\rho_{xx}) \simeq \rho_{AH}/\rho_{xx}^2$ since $\rho_{AH} \ll \rho_{xx}$.[22] The value of the σ_{AH} is obtained with the ρ_{xx} at zero magnetic field because the latter one changes little with the magnetic field as shown below. Interestingly, the σ_{AH} and R_0 are always negative for Pd-rich samples, whereas they change sign with T for Pt-rich ones.[9] At low T, they change from positive to negative with decreasing x. Meanwhile, σ_{AH} and R_0 of Pt-rich samples show a strong T-dependence, in contrast to the Pd-rich ones. Clearly, σ_{AH} and R_0 are correlated to each other. Figure 3(c) shows that ρ_{xx} of all samples increases approximately linearly with T. The residual resistivity changes non-monotonically as a function of x with a maximum near $x = 0.6$, suggesting almost random distribution of Pt and Pd atoms.[23] The ρ_{xx} of all samples falls in the region of 20–35 $\mu\Omega$ cm, further indicating high quality of the present samples.

Figure 4(a) shows the T-dependence of the AMR ratio for various x. Two distinguished features are observed. (1) The AMR ratio decreases when x drops, demonstrating the change of SOC with x. (2) The $\Delta\rho_{xx}/\rho_{xx}$ varies non-monotonically with T for Pt-rich Pd-Pt/YIG and also in Pd/YIG. The maximal value is located near 60 K for Pd/YIG; and it shifts from 120 K for Pt/YIG to lower temperatures for Pd-Pt/YIG systems,[11] different from monotonic changes of the AMR in most ferromagnets. In order to understand this phenomenon, the magnetic susceptibilities of bulk Pt and Pd were measured. Figure 4(b) shows that the susceptibilities of bulk Pt and Pd also change non-monotonically with T. Furthermore, the peak of the AMR ratio in either Pt/YIG or Pd/YIG locates at the *same* temperature for the maximal χ of the corresponding bulk metal, as highlighted by vertical dashed lines. One expects that the induced magnetization in a paramagnet is correlated to its magnetic susceptibility. The coincidence of the maximal temperature between the AMR and the χ hence further proves the presence of the MP-induced magnetization in the PdPt layer. The vanishing non-monotonic change of the AMR ratio for intermediate x may be due to the dominant effect of the impurity scattering, as demonstrated by the maximal residual resistivity near $x = 0.6$ in Fig. 3(c). Moreover, the AMR ratio in the present Pt/YIG samples is about two times larger than the results of the SMR model.[15] Finally, the in-plane angular dependence of the AMR at room temperature can be fitted by a linear function of $\cos^2\phi_H$. At the angle between the H and the sensing current $\phi_H = 0°$ the ρ_{xx} is larger than that of ρ_{xx} at $\phi_H = 90°$, in the same way for conventional magnetic metallic films,[11] as shown in Figs. 4(c) and 4(d).

To better understand the nature of the observed AHE in the Pt/YIG and Pd/YIG, we perform *ab initio* band structure calculations of the AHC in the MP-induced ferromagnetic Pt and Pd within the magnetic moment-constrained spin-density functional theory.[24] Indeed, the calculated intrinsic AHC for the induced magnetic moment up to 0.25 μ_B is positive for Pt and negative for Pd, in good agreement with the present experimental results. Interestingly, further theoretical analysis of the calculated exchange splitting (Δ_{ex}) of the energy bands and the AHC as a function of the induced spin magnetic moment (m_s) show[24] that the AHC in a MP-induced ferromagnet can be related to the energy derivative of the spin Hall conductivity (SHC, σ_{SH}) at the Fermi level (E_F) as $\sigma_{AH} \approx \Delta_{ex}\frac{e}{\hbar}\sigma_{SH}(E_F)'$. It can be seen in Refs. 25 and 26 that $\sigma_{SH}(E_F)'$ is positive for nonmagnetic Pt and is negative for nonmagnetic Pd. This intriguingly explains the subtle sign change when the Pd in Pd/YIG is replaced by Pt.

The *ab initio* calculations also show that Δ_{ex} is proportional to m_s, i.e., $\Delta_{ex}(m_s) = [\Delta_{ex}(m_s^0)/m_s^0]m_s$. Therefore,[24] we have $\sigma_{AH} \approx [\frac{e}{\hbar}\frac{\Delta_{ex}(m_s^0)}{m_s^0}\sigma_{SH}(E_F)']m_s = \gamma m_s$. Using the calculated $\sigma_{SH}(E_F)'$ and also $\Delta_{ex}(m_s^0)$ for $m_s^0 = 0.1\,\mu_B$, we obtain

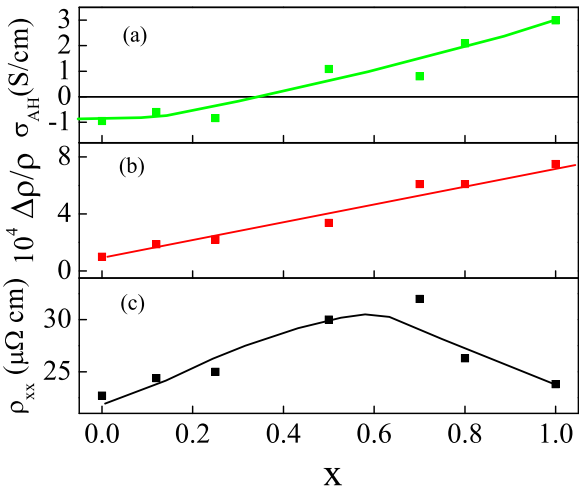

FIG. 5. For PdPt (1 nm)/YIG films, σ_{AH} (a), AMR ratio (b), and ρ_{xx} (c) versus x at 10 K. Solid lines serve a guide to the eye.

$\gamma = 788$ and -2921 S/(cm · μ_B) for Pt and Pd, respectively. Using the measured AHC in Pt/YIG (3 S/cm) and in Pd/YIG (-1 S/cm) [Fig. 5(a)], we obtain an approximate m_s value of 0.004 μ_B/atom for Pt in Pt/YIG and of 0.0003 μ_B/atom for Pd/YIG. The smallness of this estimated Pt magnetic moment perhaps explains why the induced magnetic moment was not detected in a previous XMCD experiment on Pt/YIG.[17] Nonetheless, the estimated Pt magnetic moment is several times smaller than the previously calculated value of ~0.02 μ_B (Ref. 10) and also the measured one of 0.076 μ_B by another XMCD experiment.[11] The diverse values of the Pt magnetic moment reported in the literature may reflect the fact that the MP effect in Pt is oscillatory[10] and is sensitive to the morphology at the interface.[11,17] For example, the Pt/YIG samples in the present work and Ref. 15 have very different longitudinal resistivities (20–35 $\mu\Omega$ cm vs. 50–100 $\mu\Omega$ cm), and the MP effect also differs in previous work.[11,17] Since the inclusion of the MP effect changes the interpretation of magnetotransport data from the conventional AMR, AHE, SSE[8–11] to SMR,[12–15,17] the clear identification of the MP effect in high quality PdPt/YIG samples is important for the disentanglement of different factors in observations. Moreover, the MP effect also produces sizeable spin polarization for the states of Pt around the Fermi level.[10]

Significant SOC effect on the AMR in PdPt/YIG can be seen in Fig. 5(b). At 10 K, the AMR ratio is 8.0×10^{-4} for Pt/YIG and 1.0×10^{-4} for Pd/YIG. In principle, the AMR ratio in ferromagnetic materials arises from the *s-d* scattering and is proportional to the square of the SOC strength (ξ^2), since the resistivity ratio of the spin-up and spin-down channels is fixed according to the perturbation theory.[27] Therefore, the ratio of the AMR between the Pt/YIG and Pd/YIG should be close to that of ξ^2 in the Pt and Pd layers. For intermediate x, the AMR ratio may deviate from the quadratic dependence due to the significant contributions from the composition-disorder scattering, as shown in Fig. 5(c). Therefore, the present results not only show the intriguing SOC-tuning effect on the AMR and AHE in the PdPt/YIG bilayer but also help to clarify the mechanism of the magnetotransports in these systems, thus paving the way for the promising applications of the PdPt/YIG bilayers in spintronic devices.

This work was supported by the National Science Foundation of China Grant Nos. 11374227, 51331004, 51171129, and 51201114, Shanghai Committee Nos. 0252nm004, 13XD1403700, and 13520722700), the National Science Council of Taiwan Grants (G.Y.G.), and DOE-BES Grant No. DE-FG02-05ER46237 (R.W.).

[1]J. E. Hirsch, Phys. Rev. Lett. **83**, 1834 (1999).
[2]Y. K. Kato, R. C. Myers, A. C. Gossard, and D. D. Awschalom, Science **306**, 1910 (2004).
[3]F. J. Jedema, H. B. Heersche, A. T. Filip, J. J. A. Baselmans, and B. J. van Wees, Nature (London) **416**, 713 (2002).
[4]S. O. Valenzuela and M. Tinkham, Nature (London) **442**, 176 (2006).
[5]K. Ando, Y. Kajiwara, S. Takahashi, S. Maekawa, K. Takemoto, M. Takatsu, and E. Saitoh, Phys. Rev. B **78**, 014413 (2008).
[6]E. Saitoh, M. Ueda, H. Miyajima, and G. Tatara, Appl. Phys. Lett. **88**, 182509 (2006).
[7]F. D. Czeschka, L. Dreher, M. S. Brandt, M. Weiler, M. Althammer, I. M. Imort, G. Reiss, A. Thomas, W. Schoch, W. Limmer, H. Huebl, R. Gross, and S. T. B. Goennenwein, Phys. Rev. Lett. **107**, 046601 (2011).
[8]S. Y. Huang, W. G. Wang, S. F. Lee, J. Kwo, and C. L. Chien, Phys. Rev. Lett. **107**, 216604 (2011).
[9]S. Y. Huang, X. Fan, D. Qu, Y. P. Chen, W. G. Wang, J. Wu, T. Y. Chen, J. Q. Xiao, and C. L. Chien, Phys. Rev. Lett. **109**, 107204 (2012).
[10]D. Qu, S. Y. Huang, J. Hu, R. Q. Wu, and C. L. Chien, Phys. Rev. Lett. **110**, 067206 (2013).
[11]Y. M. Lu, Y. Choi, C. M. Ortega, X. M. Cheng, J. W. Cai, S. Y. Huang, L. Sun, and C. L. Chien, Phys. Rev. Lett. **110**, 147207 (2013).
[12]T. Kikkawa, K. Uchida, Y. Shiomi, Z. Qiu, D. Hou, D. Tian, H. Nakayama, X. F. Jin, and E. Saitoh, Phys. Rev. Lett. **110**, 067207 (2013).
[13]H. Nakayama, M. Althammer, Y. T. Chen, K. Uchida, Y. Kajiwara, D. Kikuchi, T. Ohtani, S. Geprägs, M. Opel, S. Takahashi, R. Gross, G. E. W. Bauer, S. T. B. Goennenwein, and E. Saitoh, Phys. Rev. Lett. **110**, 206601 (2013).
[14]N. Vlietstra, J. Shan, V. Castel, and B. J. van Wees, Phys. Rev. B **87**, 184421 (2013).
[15]M. Althammer, S. Meyer, H. Nakayama, M. Schreier, S. Altmannshofer, M. Weiler, H. Huebl, S. Geprägs, M. Opel, R. Gross, D. Meier, C. Klewe, T. Kuschel, J. M. Schmalhorst, G. Reiss, L. M. Shen, A. Gupta, Y. T. Chen, G. E. W. Bauer, E. Saitoh, and S. T. B. Goennenwein, Phys. Rev. B **87**, 224401 (2013).
[16]Y. Y. Sun, H. C. Chang, M. Kabatek, Y. Y. Song, Z. H. Wang, M. Jantz, W. Schneider, M. Z. Wu, E. Montoya, B. Kardasz, B. Heinrich, S. G. E. te Velthuis, H. Schultheiss, and A. Hoffmann, Phys. Rev. Lett. **111**, 106601 (2013).
[17]S. Geprägs, S. Meyer, S. Altmannshofer, M. Opel, F. Wilhelm, A. Rogalev, R. Gross, and S. T. B. Goennenwein, Appl. Phys. Lett. **101**, 262407 (2012).
[18]N. E. Christensen, J. Phys. F: Met. Phys. **8**, L51 (1978).
[19]Y. Y. Sun, Y. Y. Song, H. C. Chang, M. Kabatek, M. Jantz, W. Schneider, M. Z. Wu, H. Schultheiss, and A. Hoffmann, Appl. Phys. Lett. **101**, 152405 (2012).
[20]P. T. Bao, W. X. Li, W. K. Yeoh, X. Y. Cui, J. H. Kim, Y. M. Kang, W. R. Yang, S. X. Dou, S. P. Ringer, and R. K. Zheng, Appl. Phys. Lett. **102**, 092405 (2013).
[21]Y. Q. Zhang, N. Y. Sun, R. Shan, J. W. Zhang, S. M. Zhou, Z. Shi, and G. Y. Guo, J. Appl. Phys. **114**, 163714 (2013).
[22]N. Nagaosa, J. Sinova, S. Onoda, A. H. MacDonald, and N. P. Ong, Rev. Mod. Phys. **82**, 1539 (2010).
[23]P. Blood and D. Greig, J. Phys. F: Met. Phys. **2**, 79 (1972).
[24]G. Y. Guo, Q. Niu, and N. Nagaosa, Phys. Rev. B **89**, 214406 (2014).
[25]G. Y. Guo, S. Murakami, T.-W. Chen, and N. Nagaosa, Phys. Rev. Lett. **100**, 096401 (2008).
[26]G. Y. Guo, J. Appl. Phys. **105**, 07C701 (2009).
[27]A. P. Malozemoff, Phys. Rev. B **34**, 1853 (1986).